Pflügers Arch – Eur J Physiol (2000) 439:349–355
Digital Object Identifier (DOI) 10.1007/s004249900121

ORIGINAL ARTICLE

S. Rao · S.K. Sikdar

Modification of α subunit of RIIA sodium channels by aconitine

Received: 26 April 1999 / Received after revision: 21 June 1999 / Accepted: 7 July 1999 / Published online: 2 October 1999

Abstract The effect of aconitine (AC), an alkaloid toxin, on the electrophysiological properties of the rat brain type IIA α subunit expressed heterologously in the Chinese Hamster Ovarian (CHO) cell line was studied under the whole-cell patch-clamp configuration. The activation threshold of modified channels shifted by about –40 mV. As the number of depolarizations increased, the transient current at 0 mV decreased and, in proportion, the AC-modified current at –50 mV increased. This suggests a transition of channels to an AC-modified state. The rate of modification was nearly four times faster when 50 μM AC was applied internally than when applied in the bath solution. This supports the idea that the AC-binding site is located close to the cytoplasmic mouth of the channel pore. The AC-modified sodium currents inactivated completely, although with slower kinetics. The steady-state inactivation followed a simple Boltzmann function. AC-modified currents activated without a sigmoidal delay. The permeability of the NH_4^+ ion was enhanced such that its permeability ratio increased from an initial value of 0.18 to 0.95 and for Cs^+ it was enhanced from 0.03 to 0.07. These studies show that the AC-binding site resides at the pore region of the α subunit of the Na^+ channel, and that the presence of β subunit/s is not essential for AC binding.

Key words Aconitine · Accessibility to aconitine receptor · Kinetics · Rat brain type IIAα subunit · Whole-cell patch clamp

Introduction

Aconitine (AC) belongs to the group of lipid-soluble "alkaloid toxins" along with batrachotoxin, veratridine and grayanotoxin, which are known to act at a common receptor (site 2) on the voltage-gated sodium channel [1]. It is derived from the plant *Aconitum napellus*. These alkaloids are powerful modifiers of the voltage-gated sodium channel. They affect all properties of the channel, namely activation, inactivation, selectivity, and susceptibility to various drugs and toxins [2]. Therefore, they have proven to be important tools in studies aiming to elucidate channel structure and function.

AC interacts with open channels and brings about very stable modification [3]. It causes a negative shift in the voltage dependence of activation and a pronounced decrease in the selectivity of Na^+ in various cells: in cardiac muscle, myelinated nerves, frog skeletal muscle and neuroblastoma cells. Its effect on channel inactivation varies in different preparations – elimination of inactivation [4] or partial inactivation [5] in AC-modified channels in the myelinated nerve fibres of *Xenopus laevis*, more pronounced inactivation in frog skeletal muscle [6] and near-normal inactivation in neuroblastoma cells [7].

The above-mentioned studies were performed on preparations expressing channels in their native state. This study concerns the electrophysiological and some kinetic properties of the α subunit of rat brain IIA (RIIA) sodium channels, expressed heterologously in isolation, in a somatic cell line, upon modification by AC. Previous work in our laboratory [8] has shown that the untransfected Chinese Hamster ovary (CHO) cell line does not contain any endogenous voltage-gated channels that could interfere with our current recordings. We investigated the trend of AC modification as a function of depolarizing pulse number, which also allowed us to deduce the accessibility of the AC receptor to its ligand.

Materials and methods

CHO cells stably expressing the RIIA sodium channel α subunit, CNa18 cells [8], were cultured in Dulbecco's modified Eagle's medium (DMEM) and F12 Ham mixture supplemented with 8% fetal bovine serum in the presence of 225 μg/ml G418 antibiotic in a humidified 5% CO_2 environment. These cells were put into 35-mm-diameter dishes, grown to 40–60% confluence and used for whole-cell patch-clamp recordings.

S. Rao · S.K. Sikdar (✉)
Molecular Biophysics Unit, Indian Institute of Science,
Bangalore 560012, Karnataka, India
e-mail: sks@mbu.iisc.ernet.in
Fax: +91-080-3348535

Bath solutions contained (in mM): 137 NaCl or 135 NH_4Cl; 5 HEPES; 1 $MgCl_2$; 1.5 $CaCl_2$; 10 glucose. pH was adjusted to 7.4 using NaOH. Pipette solution contained (in mM): 24 NaCl; 116 CsCl; 10 HEPES; 10 EGTA and 0.5 $CaCl_2$. Symmetrical sodium solutions were used in the experiment where AC was added internally.

To study the effect of increasing pulse number on both the transient sodium current (I_{peak}) and the AC-modified current (I_{mod}), a two-pulse protocol was used (Fig. 3). The first pulse was a step to 0 mV from a holding potential of –90 mV, and the second pulse was to –50 mV to record currents only from AC-modified channels. To obtain well leak-subtracted I_{mod} at –50 mV of small magnitude, we used a simple voltage protocol consisting of four test pulses to –50 mV and ten leak pulses of one-fourth its amplitude in the hyperpolarizing direction alternating with the double-pulse protocol. The pulse number was varied from 0 to 2000.

A 5 mM stock solution of AC (obtained from Sigma, St. Louis, Mo., USA) was prepared using acidified bath solution, to dissolve the AC, and then the pH was raised to 7.4.

A final concentration of 50 µM AC, applied externally or internally, was used during the measurement of the current–voltage relationships for the AC-treated channels. The holding potential was set at –100 mV or –90 mV. As reported previously the rate of onset of AC's effects depends on the stimulation [2]. Depolarizing pulses of 7 ms duration to 0 mV were applied at 10 Hz to modify the channels with AC.

Data acquisition and analysis

Pipettes were pulled from thin-walled glass capillaries (1.5 mm o.d., 1.17 mm i.d., Intracel, Royston, Herts, UK) in a two-stage pulling procedure using a vertical puller (Model P-30, Sutter Instrument) and fire polished. Pipettes filled with the pipette solution had a resistance of 1–1.5 MΩ. After establishing the whole-cell mode, cells were voltage-clamped to –100 mV or –90 mV using a List EPC-7 patch-clamp amplifier. Capacitance and series resistance compensation (up to 70%) was achieved using the built-in circuits of the EPC-7 amplifier.

Signals were filtered at 3 kHz, (low-pass, Bessel 3-pole) and acquired at 16 kHz using an A/D converter (CED 1401, Cambridge, UK). Application of pulse protocols, leak correction and data analysis were done using the WCP program provided by John Dempster (University of Strathclyde, UK). SigmaPlot version 1.02 (Jandel Scientific, Calif., USA) was used for curve fitting and plotting data. Results are expressed as mean ±SEM.

AC binding

Both the decay of the transient current (I_{peak}) and the rise of I_{mod} in the binding experiments were fit to exponential functions given in Eqs. 1 and 2:

$$I=I_1 \exp(-t/\tau)+I_2 \quad (1)$$

(for decaying I_{peak}), and

$$I=I_1[1-\exp(-t/\tau)]+I_2 \quad (2)$$

(for rising I_{mod}), where the constant $\tau=-1/\ln(1-F)$ is given in terms of pulse number [9]. F is either the fractional decrease or fractional increase of current per pulse in this instance, or the fractional modification per pulse. τ was kept as a free parameter in the fits. The value of F was calculated from the expression after substitution of the τ value obtained from the fits. I_1 and I_2 are the current amplitudes; t is the pulse number.

Conductance–voltage relationship

The voltage dependence of conductance was fit with a Boltzmann function of the form shown in Eq. 3:

$$g_{Na}=1/\{1+\exp[(V-V_{1/2})/k]\} \quad (3)$$

where g_{Na} is the conductance, V the test voltage, $V_{1/2}$ the voltage at half-maximal conductance and k the slope factor.

Waveform analysis

A method of analysis similar to that employed for the wild-type channel currents [10] was used. The following forms of the Hodgkin–Huxley equation (Eqs. 4, 5) were used to fit the I_{mod} waveform at potentials of –70 mV, –60 mV and –50 mV.

$$I_{Na}(t)=\{1-\exp[-(t-\delta t)/\tau_m]\}^x \cdot \{[I_1\exp(-t/\tau)+I_2]\} \quad (4)$$

and

$$I_{Na}(t)=\{1-\exp[-(t-\delta t)/\tau_m]\}^x \cdot \{[I_1\exp(-t/\tau_1)+I_2\exp(-t/\tau_2)+I_3]\} \quad (5)$$

at higher potentials, where δt is the instrumental delay and was kept as a free parameter in the fitting equation. τ_m is the time constant of activation. τ_1 and τ_2 are the fast and slow time constants of inactivation respectively.

Steady-state inactivation

The voltage dependence of the steady-state inactivation was fit by a Boltzmann function (Eq. 6) of the form:

$$h_\infty=1/\{1+\exp[(V-V_{1/2})/k]\} \quad (6)$$

where h_∞ is the probability of the channels being in the non-inactivated state, V is the test voltage, $V_{1/2}$ the voltage of half inactivation and k the slope factor.

Selectivity

The permeability ratio $P_{NH_4^+}/P_{Na^+}$ for modified channels was calculated from the Goldman-Hodgkin-Katz (GHK) voltage equation (Eq. 7) [11]:

$$E_{rev}=\frac{RT}{zF}\ln\frac{P_{Na^+}[Na^+]_{out}+P_{NH_4^+}[NH_4^+]_{out}}{P_{Na^+}[Na^+]_{in}+P_{Cs^+}[Cs^+]_{in}} \quad (7)$$

E_{rev} is the observed reversal potential, RT/zF being a constant at a particular temperature. , $P_{NH_4^+}$ and P_{Cs^+} are the permeabilities of Na^+, NH_4^+ and Cs^+ ions respectively. The ratio P_{Cs^+}/P_{Na^+} for modified channels was computed using the simplified GHK equation with 137 mM Na^+ present in the external solution and 116 mM Cs^+ in the internal solution.

Result

Figure 1 illustrates a family of currents recorded at five potentials from a single cell before (Fig. 1A) and after (Fig. 1B) treatment with 200 µM AC. A hyperpolarizing shift in the activation threshold is obvious in Fig. 1B. It is noteworthy that the current amplitudes at –70, –60, –50 and –40 mV are greater compared with the control, indicating that the currents at these potentials are mostly derived from the AC-modified fraction of channels. Also seen is a considerable reduction in the current amplitude at –30 mV. The peak current amplitude of unmodified currents was suppressed up to 70% upon modification with AC (current traces at all potentials not shown).

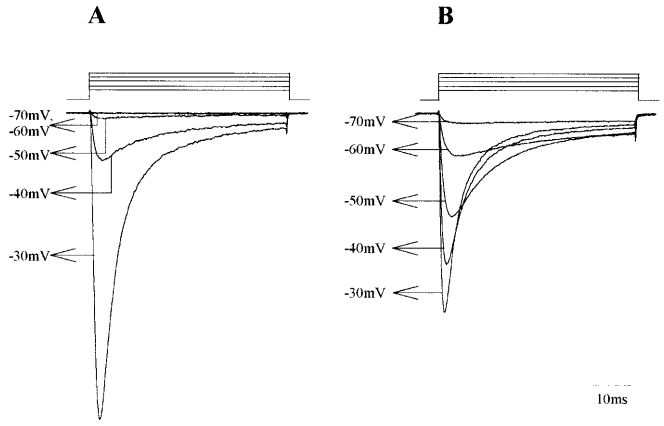

Fig. 1A,B Family of currents recorded from a single cell at potentials (in mV) of –70, –60, –50, –40 and –30. V_{hold}=–100 mV, and pulse duration is 50 ms. **A** Before aconitine (*AC*) treatment, and **B** upon external addition of 200 µM AC and following stimulation with 1500 depolarizing pulses at a frequency of 10 Hz. The currents are normalized with respect to the maximal peak current in **A**

Figure 2A shows the normalized peak current–voltage relationship of AC-modified channels superimposed over the control. It shows a shift in the activation threshold of modified channels by about 40 mV and a shift by 10 mV in the current peak in the hyperpolarizing direction. A negative shift in the reversal potential for AC-modified currents is seen, indicating that the channel selectivity is altered.

Figure 2B shows the voltage dependence of conductance for the AC-modified and unmodified channels. It follows a Boltzmann distribution (Eq. 3) with $V_{1/2}$=–28.69 mV and k=–11 mV for the modified and $V_{1/2}$=–15.82 mV and k=–8.64 mV for the unmodified channels. The voltage range of activation shifted by –40 mV. The $V_{1/2}$ shifted by –13 mV, without a significant change in the steepness of voltage dependence.

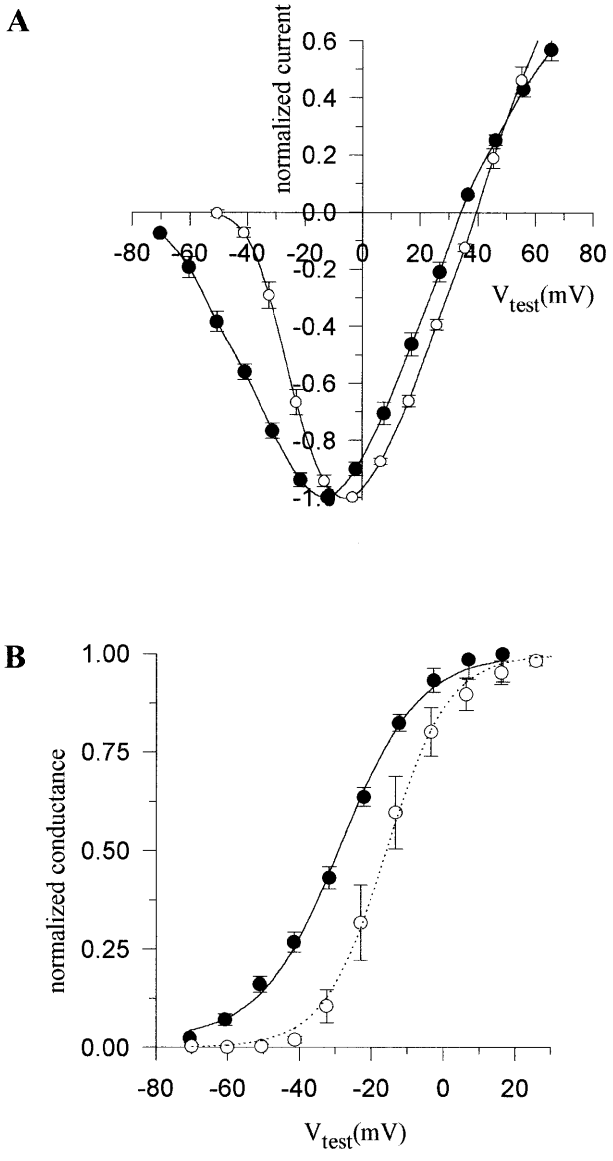

Fig. 2A Normalized current–voltage relationship of AC-modified currents (*filled circles*, n=4) superimposed over unmodified-channel currents (*open circles*, n=5). **B** Normalized conductance–voltage plot of AC-modified currents (*filled circles*, n=4) superimposed over unmodified-channel currents (*open circles*, n=3). *Solid line* represents the Boltzmann fit for the former, $V_{1/2}$=–28.69 mV, k=–11 mV, and the *dotted line* represents Boltzmann fit for the latter, $V_{1/2}$=–15.82 mV, k=–8.64 mV. *Error bars* indicate ±SEM

Effect of depolarizing pulse number on AC modification

Effect of external AC addition

The two-pulse protocol used in this experiment is illustrated in Fig. 3 (described in Materials and methods). Two superimposed current traces are shown prior to stimulation (a) and after pulsing 1000 times (b). The transient current in the first pulse is suppressed by about 70% whereas the current at –50 mV increases upon pulsing, indicating an increase in the fraction of AC-modified channels.

Figure 4A shows how I_{peak} and I_{mod} vary with pulse number in the presence of 50 µM AC in the bath solution. I_{peak} and I_{mod} were normalized to their respective maximum value. The data points fit well to exponential functions (Eqs. 1 and 2), with τ=192 and 225 pulses for I_{peak} and I_{mod} respectively. It is apparent that the progressive decrease in I_{peak} correlates well with the progressive increase in I_{mod}, the τ values being comparable. The derived value of the fractional decrease of I_{peak} per pulse, F=0.005, was comparable to the value of the fractional increase of I_{mod}, F=0.004. The I_{mod} saturates after about 1000 pulses, which indicates that almost all channels are modified by AC. The number of pulses required to attain 50% modification is approximately 200.

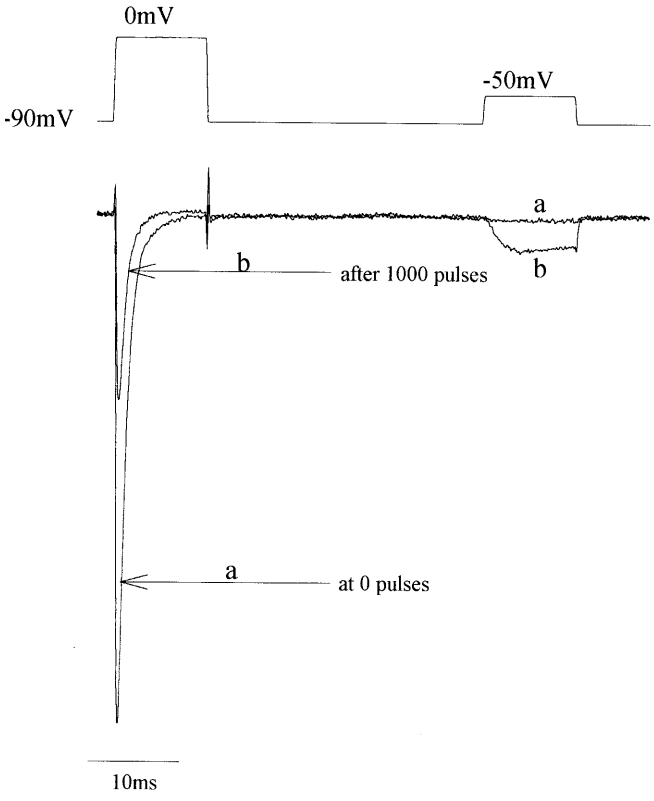

Fig. 3 Illustration of the two-pulse protocol used to follow modification following the external application of 50 μM AC. The duration of each pulse is 10 ms with a 30-ms interpulse interval. The figure shows normalized superimposed current traces (*a* and *b*) prior to stimulation and after 1000 depolarizing pulses. V_{hold}=–90 mV

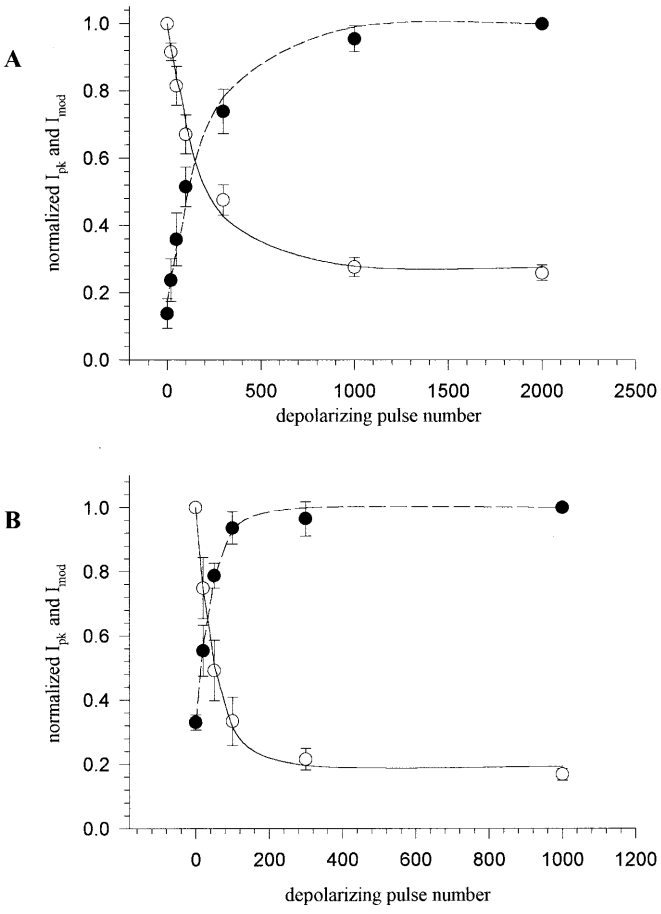

Fig. 4A,B Normalized plot of the peak transient current (I_{pk}) and AC-modified current (I_{mod} at –50 mV) as a function of depolarizing pulse number. **A** Fifty micromolar AC added externally. *Open circles* denote I_{pk} value (n=5) and *filled circles* the I_{mod} value (n=3). The *solid line* is an exponential fit through the I_{pk} values (Eq. 1), with τ=192 pulses and the fractional decrease, F, equal to 0.005 (see text). The *dashed line* is the fit through I_{mod} values (Eq. 2), with τ=225 and the fractional increase, F, equal to 0.004. **B** AC (50 μM) added via the pipette. The *symbols* denote I_{pk} (n=3) and I_{mod} (n=3) as mentioned above. Parameters of exponential fits of I_{pk} are τ=53, F=0.019 and of I_{mod} are τ=44 and F=0.02. *Error bars* denote ±SEM

Effect of internal AC addition

Figure 4B shows the effect of internal application of 50 μM AC. It is evident that the number of pulses required to modify half the channels is approximately 50, which is 4 times less than when AC is added to the external bath solution. The exponential fits of the declining I_{peak} and rising I_{mod} yielded comparable τ values of 53 and 44 respectively. In this case too, the value of the fractional decrease of I_{peak} per pulse, 0.019, was comparable to the value of the fractional increase of I_{mod}, 0.02.

This analysis clearly demonstrates that the τ values for I_{peak} and I_{mod} when AC is added to the bath are nearly 4 times greater than when it is added via the pipette. The fractional modification per pulse, F, was also approximately four times greater when AC was added internally.

Inactivation

The inactivation was described by a sum of two exponential functions (second part of Eq. 5). Figure 5A and B show the voltage dependence of the fast and the slow time constants. Currents inactivated partially at negative potentials and were better fit by a monoexponential function (second part of Eq. 4), but inactivated completely at potentials beyond –40 mV and were better fit with a biexponential function. The fast time constants for inactivation are comparable to those of the normal channels [10]. However, the slow time constants of AC-modified channels were found to be about 11.5±1.5 times the fast time constants at all potentials, whereas those of the unmodified channels were no more than 5 times faster [10]. This indicates that AC slows down inactivation.

The steady-state inactivation (h_∞) of AC-modified channels (Fig. 6) was determined using a two-pulse protocol with a 500-ms-long conditioning prepulse, from V_{hold}=–100 mV, varying from –130 mV to –10 mV in 7-mV steps followed by a test pulse of 15 ms duration to 0 mV. The steady-state inactivation was well fit by a Boltzmann function (Eq. 6) with $V_{1/2}$=–67.17 mV and k=5.6 mV. $V_{1/2}$ was shifted in the hyperpolarizing direction by 15 mV compared to the normal channels [10]. The steepness of

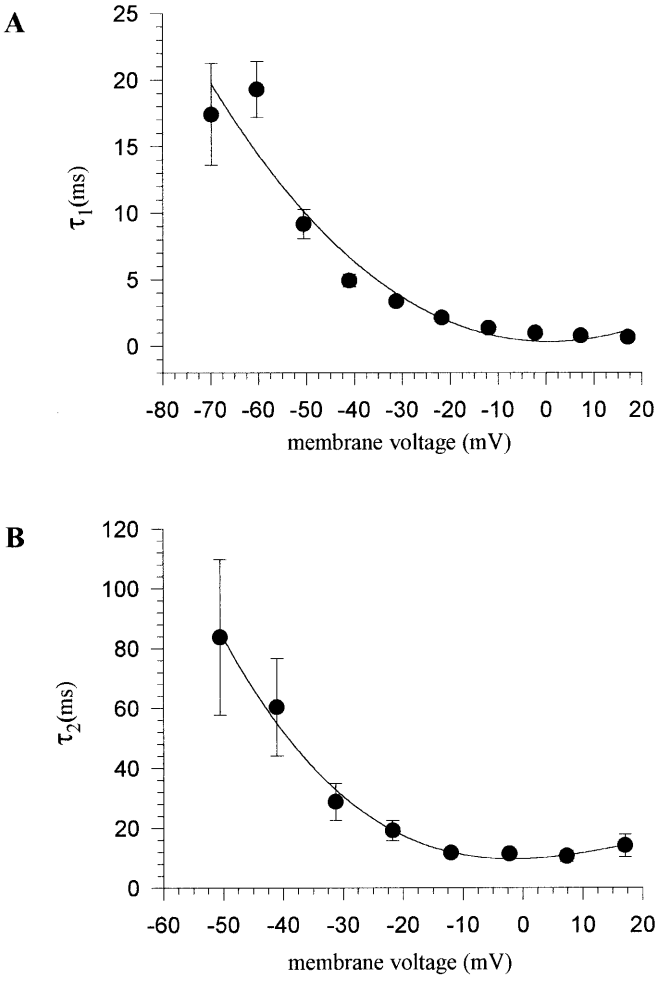

Fig. 5A,B Potential dependence of the time constants of inactivation of AC-modified currents. **A** Potential dependence of the fast time constant, τ_1 (n=4). **B** Potential dependence of the slow time constant, τ_2 (n=4). *Filled symbols* indicate the time constant values at that potential in both the above figures. *Error bars* denote ±SEM. *Solid lines* through data points denote lines of regression

Table 1 Best value of power x, after fitting activation with an exponential function of the form $\{1–\exp[–(t-\delta t)/\tau_m]\}^x$ at different potentials. Values from 8 cells, along with mean ±SEM are shown.

Cell	Max I_{Na} (pA)	x at membrane potential (mV)				
		–70	–60	–51	–41	–30
s3007a2	9189	0.62	1.04	1.44	1.55	1.39
s1708a1	4504	0.65	1.11	1.27	1.54	1.86
s0809a1	6636	0.53	0.93	1.52	1.69	1.87
s0308b2	3523	0.58	0.87	0.84	1.65	1.26
s1306a4	3938	0.88	1.25	1.18	1.44	2.22
s2306a1	3784	0.76	1.27	1.40	1.41	2.22
s1808a2	1050	0.61	0.77	0.99	0.84	1.16
s3008a1	3328	0.48	0.82	1.07	1.10	1.39
Mean	4494	0.64	1.01	1.22	1.40	1.67
SEM	862	0.04	0.07	0.08	0.10	0.15

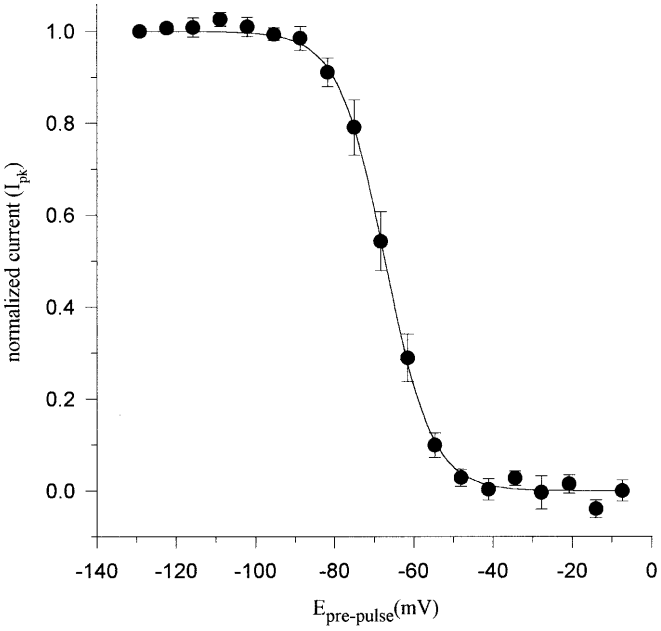

Fig. 6 Steady-state inactivation curve of AC-modified channels. *Filled symbols* are the data points (n=7). *Line* drawn through the data points is a Boltzmann fit (Eq. 3), the parameters being $V_{1/2}$=–67.17 mV and k=5.89 mV. *Error bars* denote ±SEM

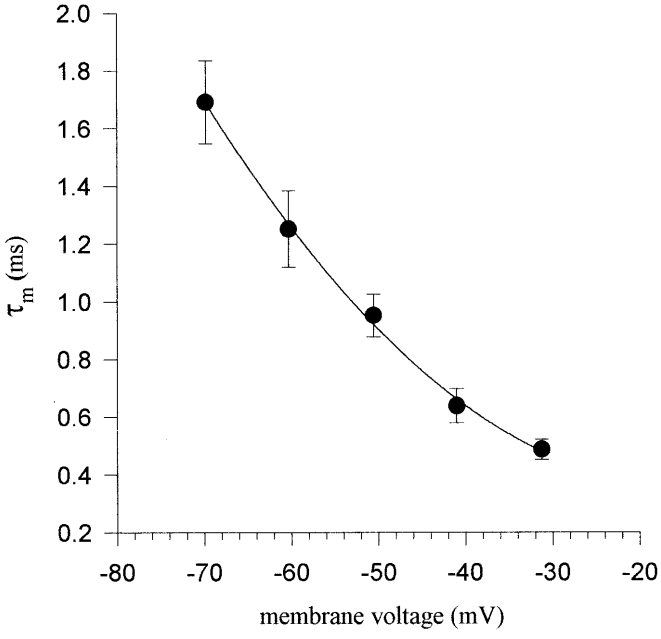

Fig. 7 Potential dependence of activation time constant (τ_m) of AC-modified channels. *Filled symbols* are the data points (n=7). *Error bars* denote ±SEM. A regression line is drawn through the data points

voltage dependence was not significantly different from k, which was 4.7 mV for normal channels.

Activation

Activation was described by an exponential function raised to the power x (first part of Eqs. 4 and 5). The val-

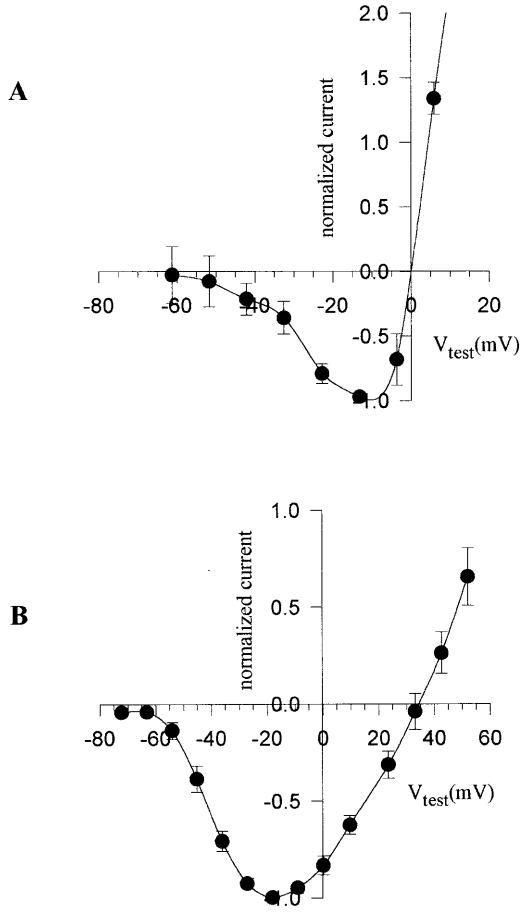

Fig. 8A,B Normalized current–voltage relationship of ammonium currents. **A** Unmodified channels (*n*=3); **B** AC-modified channels (*n*=5). *Error bars* denote ±SEM

ues of the power *x* for potentials –70 mV to –30 mV, where most of the unmodified channels remain shut, are indicated in Table 1. The values are seen to vary between 1 and 1.5. Figure 7 shows the potential dependence of the time constants of activation. The range of potentials (–70 mV to –30 mV) was selected to eliminate any contaminating current from unmodified channels.

Selectivity

AC brings about a considerable reduction in the selectivity of the channel for Na^+. The channel, on the other hand, becomes highly permeable to NH_4^+ [5, 6, 7] and has greater permeability to Cs^+. Any change in the selectivity of the channel is reflected by a change in the E_{rev} for the ion in question. Fig. 8A, B illustrates experiments in which Na^+ in the bath solution was replaced by equimolar NH_4^+(135 mM). Figure 8A shows the peak current–voltage relationship of NH_4^+ current through the unmodified channels, where the E_{rev} is 0 mV. After maximum modification the reversal for NH_4^+ current shifted by +35 mV (Fig. 8B). The GHK voltage equation was used to compute the permeability ratios of Cs^+ and NH_4^+ ions for the AC-modified channels from the observed E_{rev} (Eq. 7). The permeability ratio of Cs^+ was determined to be 0.07, from an initial value of 0.03. The relative permeability of NH_4^+ was determined to be 0.95 from an initial value of 0.18.

Discussion

Our studies performed on the heterologously expressed α subunit of the RIIA sodium channel revealed that AC modifies its properties, so that they become similar to those of AC-modified Na^+ channels of neuroblastoma cells [7] in terms of apparent completeness of inactivation and permeability. Though our cells did not have any β subunits, AC modified the channels in a way that has been reported for the various preparations expressed in their native state. Therefore, the presence of β subunits does not appear to be essential for AC binding.

Since AC-modified channels are able to inactivate, and the shift in the activation threshold is narrow, it is impossible to distinguish pharmacologically between the modified and unmodified channel populations at all potentials.

The approximately 70% reduction in the amplitude of the transient current may be due to a decrease in the single-channel conductance of the modified channels. The blocking action of AC on the unmodified channel proposed by Caterall [1] still remains unclear.

Increasing the number of pulses applied to AC-treated cells saturates I_{peak} and I_{mod}. Therefore, we can assume that almost complete modification of channels has occurred at saturation, and that only a small fraction of current from unmodified channels remains. Therefore, our description of the kinetic and steady-state properties of AC-modified currents upon stimulating the cell repetitively until saturation is fairly reliable. However, we remain uncertain about the precise number of unmodified channels remaining at the saturation point.

The rate of onset of modification with pulse number depends on the route of administration of AC. The data suggest that AC is able to access its binding site approximately four times faster when administered internally than when added to the bath. This strongly suggests that AC's binding site is located towards the cytoplasmic mouth of the channel pore.

Inactivation

Inactivation is incomplete at potentials of –70 to –50 mV. At higher potentials the currents inactivate completely, and this is alteredby AC. This is reflected in the increase in the slow time constants of inactivation following application of AC.

The steady-state inactivation shows a two-state distribution as against the three-state distribution for the unmodified channels [10]. This suggests that AC abolishes one of the two steady-state inactivation states. More rigorous study is needed to clarify these results. The hyper-

polarizing shift in h_∞ suggests that AC-modified channels recover from inactivation more slowly than unmodified channels.

Activation

The activation analysis indicates that AC, like all other alkaloid toxins, makes the channels activate more quickly. The sigmoidal delay undergone by the unmodified channels does not occur. Unmodified channel activation is controlled by the movement of two activation particles; however, in the AC-modified channels it appears to be controlled by the movement of a single activation particle.

Selectivity

The structure of the K^+ channel of *Streptomyces lividans* (KcsA) revealed by Doyle et al. [12] describes the presence of a sheet of hydrophobic amino acids around the selectivity filter that are essential for its structural integrity. The voltage-dependent Na^+ channel probably has similar structural elements at its pore region, since a distant homology exists between K^+ and Na^+ channels, especially at the regions involved in selectivity function. We speculate that the effects of AC on channel selectivity are due to a widening of the pore brought about by its binding at a hydrophobic region close to the pore that is important in the maintenance of the conformation at the selectivity filter region of the pore.

Mechanism of action of AC

The above-discussed effects of AC can be explained by its binding stably to a region on the sodium channel that is important for the normal functioning of the channel. Our experiments suggest that AC may bind close to the channel pore. Soldatov et al. [13] have shown the involvement of lipid components in batrachotoxin binding. However, increasing evidence is accumulating in favour of the channel pore being the region of binding for the site 2 toxins rather than the protein–lipid interface. The earlier study by Ghatpande and Sikdar [14] showed that there is a mutually exclusive binding interaction between veratridine and the open channel blocking peptide KIFMK. Wang and Wang [15] showed that a mutation in the DI-S6 region of the channel renders it insensitive to batrachotoxin. The alkaloid toxins share a common receptor, which is a strong indication that their sites of binding are at the pore region. However, the binding site remains obscure and is yet to be characterized. The effect of other open channel blockers on the binding of a toxin like AC would indeed provide greater insights into its mechanism of action.

Acknowledgements S. Rao is a Senior Research Fellow of CSIR, India. This research was supported by grants from the Department of Science and Technology (D.S.T), India. We thank A.S. Ghatpande for valuable comments and discussions. The equipment was partly financed by the Erna & Victor Hasselblad Foundation, Sweden.

References

1. Catterall WA (1977) Activation of the action potential Na^+ ionophore by neurotoxins. An allosteric model. J Biol Chem 252:8669–8676
2. Khodorov BI (1985) Batrachotoxin as a tool to study voltage-sensitive sodium channels of excitable membranes. Prog Biophys Mol Biol 45:57–148
3. Naumov AP (1983) Modification of sodium channel with scorpion toxins and alkaloids. In: Hucho F, Ovachinnikov Yu (eds) Toxins as tools in neurochemistry. de Gruyter, Berlin, pp 13–23
4. Schmidt H, Schmitt O (1974) Effects of aconitine on the sodium permeability of the node of Ranvier. Pflügers Arch 349: 133–148
5. Mozhayeva GN, Naumov AP, Negulayev Yu, Nosyreva ED (1977) The permeability of aconitine-modified sodium channels to univalent cations in myelinated nerve. Biochim Biophys Acta 466:461–473
6. Campbell DT (1982) Modified kinetics and selectivity of sodium channels in frog skeletal muscle fibres treated with aconitine. J Gen Physiol 80:713–731
7. Grishchenko I, Naumov AP, Zubov AN (1983) Gating and selectivity of aconitine-modified sodium channels in neuroblastoma cells. Neuroscience 9:549–554
8. Sarkar SN, Sikdar SK (1994) High level stable expression of rat brain type IIA sodium channel α subunit in CHO cells. Curr Sci 67:196–199
9. Hessler NA, Shirke AM, Malinow R (1993) The probability of transmitter release at a mammalian central synapse. Nature 366:569–572
10. Sarkar SN, Adhikari A, Sikdar SK (1995) Kinetic characterization of rat brain type IIA sodium channel α subunit stably expressed in CHO cells. J Physiol (Lond) 488:633–645
11. Hille B (1992). Ionic channels of excitable membranes, 2nd edn. Sinauer, Sunderland, Mass.
12. Doyle DA, Cabral JM, Pfuetzner RA, Kuo A, Gulbis M, Cohen SL, Chait BT, MacKinnon R (1998) The structure of the potassium channel: molecular basis of K^+ conduction and selectivity. Science 280:69–77
13. Soldatov N, Prasolova T, Kovalenko V, Petrenko A, Grishin E, Ovachinnikov Yu (1983) Identification of sodium channel components interacting with neurotoxins. In: Hucho F, Ovachinnikov Yu (eds) Toxins as tools in neurochemistry. de Gruyter, Berlin, pp 13–23
14. Ghatpande AS, Sikdar SK (1997) Competition for binding between veratridine and KIFMK: an open channel blocking peptide of the RIIA sodium channel. J Membr Biol 160:177–182
15. Wang SY, Wang GK (1998) Point mutations in segment I-S6 render voltage-gated Na^+ channels resistant to batrachotoxin. Proc Natl Acad Sci USA 95:2653–2658